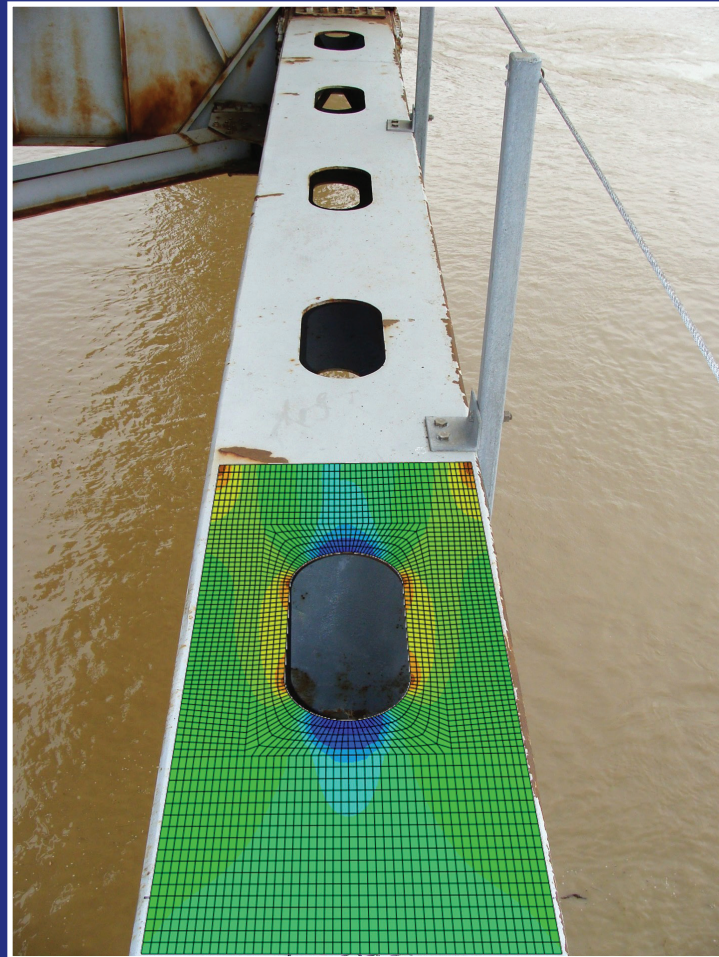


Load-Induced Fatigue Category of Hand Holes and Manholes



Francisco Javier Bonachera Martín, Robert J. Connor



RECOMMENDED CITATION

Bonachera Martín, F. J., & Connor, R. J. (2017). *Load-induced fatigue category of hand holes and manholes*. West Lafayette, IN: Purdue University. <https://doi.org/10.5703/1288284316633>

AUTHORS

Francisco Javier Bonachera Martín

Purdue University

Robert J. Connor

Purdue University

ACKNOWLEDGMENTS

The purpose of this document is to provide additional design guidance regarding the fatigue resistance associated with hand holes, manholes, and other inspection access holes typically found in box or tub steel members. The information in this document is based on an independent study conducted at the Robert L. and Terry L. Bowen Laboratory for Large-Scale Civil Engineering Research through the S-BRITE Center at Purdue University. The research described in the current document serves as background to provisions considered for implementation in the AASHTO LRFD Bridge Design Specification.

NOTICE

The contents of this document reflect the views of the authors, who are responsible for the facts and the accuracy of the data presented herein. The report does not constitute a standard, specification or regulation.

COPYRIGHT

Copyright 2017 by Purdue University. All rights reserved.

Print ISBN: 978-1-62260-482-1

ePUB ISBN: 978-1-62260-483-8

CONTENTS

1. INTRODUCTION	1
2. METHODOLOGY	2
3. RESULTS	5
4. DISCUSSION	7
4.1 Circular Holes	7
4.2 Square Holes	7
4.3 Oval Holes	7
4.4 Effect of Slots Near Inspection Access Holes	8
5. CONCLUSIONS	10
REFERENCES	12

LIST OF TABLES

Table	Page
Table 3.1 Summary of results for circular holes	5
Table 3.2 Summary of results for square holes with A/W of 0.20, 0.30, 0.40, and 0.50	5
Table 3.3 Summary of results for square holes with A/W of 0.60, and 0.70	6
Table 3.4 Summary of results for square holes with A/W of 0.80, and 0.90	6
Table 3.5 Summary of results for oval holes	7
Table 3.6 Summary of results for rectangular holes	7
Table 3.7 Summary of results for tub girder inspection access holes with adjacent slot holes	7

LIST OF FIGURES

Figure	Page
Figure 1.1 Truss diagonal showing typical hand hole details	2
Figure 2.1 Annotated sketches of manhole and hand hole geometries modeled	3
Figure 2.2 Set of geometries selected for parametric study	3
Figure 2.3 Comparison of mesh sizes used in analysis	4
Figure 2.4 Example of tub girder inspection access hole with slot hole for lock, slot hole detail highlighted	4
Figure 2.5 Annotated sketches of tub girder inspection access hole geometries modeled	4
Figure 4.1 Stress concentration factor (SCF) of circular holes	8
Figure 4.2 Stress concentration factor (SCF) of square holes with A/W of 0.20, 0.30, 0.40, and 0.50	8
Figure 4.3 Stress concentration factor (SCF) of square holes with A/W of 0.60, 0.70, 0.80, and 0.90	9
Figure 4.4 Stress concentration factor (SCF) of tub girder inspection access holes with adjacent slot holes	9
Figure 4.5 Position of slot hole and region of low tensile stress “in front of” access hole	10
Figure 5.1 Modification to Table 6.6.1.2.3-1—Detail Categories, for Load-Induced Fatigue, Section 1—Plain Material away from Any Welding on the AASHTO LRFD Bridge Design Specification	11

1. INTRODUCTION

In current bridge design specifications and evaluation manuals from the American Association of State Highway and Transportation Officials (AASHTO, 2011, 2014) the detail category for load-induced fatigue of an open hole is category D. In “Table 6.6.1.2.3-1—Detail Categories for Load-Induced Fatigue” of the AASHTO LRFD Bridge Design Specifications, a report by Brown, Lubitz, Cekov, Frank, and Keating (2007) on an experimental study undertaken to determine the effect of hole making on the behavior of steel plates and connections is provided as reference (AASHTO, 2014). However, the different specimens tested by Brown et al. (2007) were limited to 6” wide plates with 15/16” diameter holes. Although these dimensions are appropriate for the assessment of relatively small holes, such as the ones used for mechanical fastening; larger holes like access holes, such as common hand holes in built-up members, or those used for inspection access, such as for entry into steel tub girders, may have a different category for load-induced fatigue.

AASHTO groups fatigue-prone details into categories depending on its performance during fatigue testing so that the susceptibility of a detail to develop a fatigue crack can be accounted for in bridge design and evaluation (AASHTO, 2011, 2014). When a plate is subjected to uniform tension, the presence of holes, welds, etc. disrupts the stress field and results in locations in which the stress is concentrated. The severity of these stress concentrations is the main driver of fatigue damage initiation. Although other factors such as cracking mode, residual stresses, fastener pre-tension forces, etc. play an important role, in general, details with higher hot spot stress to net stress ratios have worse category for load-induced fatigue. This is particularly true for plates with open holes, as the cracking initiation point of an open hole is in the net section originating at the side of the hole (AASHTO, 2011, 2014), a location in which residual stresses do not play a role.

The ratio of the maximum stress to net stress ratio is also known as stress concentration factor. The first calculation of the stress concentration factor of a hole was performed by Kirsch (1898), who calculated the linear elastic solution for stresses around a hole in an infinite plate and computed a maximum stress concentration factor of 3. This means that a determined nominal net stress range will effectively be three times in a plate with an open hole than in a smooth plate. This effect is actually “built-in” to the AASHTO curves. For example, the constant-amplitude fatigue threshold of smooth base metal is 24 ksi (AASHTO, 2011, 2014), while the constant-amplitude fatigue threshold of an

open hole would be expected to be about 8 ksi, a factor of 3.0. This is just over 7 ksi, which is the constant-amplitude fatigue threshold of a category D detail (AASHTO, 2011, 2014), based on full-scale testing.

However, when a plate of finite dimensions is considered, the stress concentration factor decreases (Pilkey & Pilkey, 2008) due to the increased net-section stress, suggesting that when the hole diameter to plate width ratio is high, the category for load-induced fatigue may show an apparent improvement. Similarly, when the geometry of the hole is elongated, such as an ellipse or oval, the stress concentration factor also decreases (Pilkey & Pilkey, 2008). As the stress concentration factors can be directly compared with the ratios between constant-amplitude fatigue thresholds of the different categories with respect to category A, a hole which stress concentration factor is lower than 2.4 may be reasonably considered as a category C detail, and if the stress concentration factor is below 1.5 may be reasonably considered as a category B detail.

Bridge engineers and owners can benefit from a more accurate classification of open holes in the detail categories for load-induced fatigue. In tub girders it is very common to install inspection access manholes that occupy a large portion of the bottom flange of the girder, leaving a reduced net section for which assuming the current load-induced fatigue category (i.e., Category D) may be overly conservative. Similarly, it is usual to see built-up truss members in which hand holes have been placed throughout the length of the member to reduce dead load and aid with fabrication and inspection, as shown in Figure 1.1. As previously stated, designating this large openings as Category D could be overly conservative, particularly since the authors of the current report are not aware of any instances of fatigue damage in manholes or hand holes.

Based on the above, the current study will show that large open holes have lower stress concentration factors than small open holes, thereby resulting in superior fatigue resistance leading to re-classification of the detail in load-induced fatigue categories better than category D. The objectives of the current study are to (1) calculate stress concentration factors for a variety of hole geometries, (2) group hole geometries into categories for load-induced fatigue based on geometrical parameters, and (3) develop recommendations to be adopted by AASHTO in their design and evaluation specifications. To achieve the objectives, the finite element analysis (FEA) software package ABAQUS is used to conduct a parametric study in which over a hundred scenarios are analyzed.



Figure 1.1 Truss diagonal showing typical hand hole details.

2. METHODOLOGY

The first step in a parametric study is the selection of scenarios to be studied. As the main aim of this study is the calculation of stress concentration factors for a variety of hole geometries that represent typical hand holes and manholes, the following four types of geometries were selected:

1. Circular holes, as shown in Figure 2.1.
2. Square holes, with filleted corners, as shown in Figure 2.1.
3. Oval holes, composed of two semicircular holes and a rectangular intermediate section, as shown in Figure 2.1.
4. Rectangular holes, with filleted corners, as shown in Figure 2.1.

Since the stress concentration factor does not depend on the absolute value of any geometrical feature, but on the relative dimensions of the hole with respect to the plate, it is not necessary to model an array of specific plate widths, hole radiuses, etc. Instead, ratios of hole width to plate width (A/W), hole length to plate width (B/W), and radius to plate width (R/W) were selected so that sufficient cases are studied. The length of the plate utilized in the finite element models is ten times the width of the plate, which was sufficiently large to guarantee that the loading represented far-field conditions for the hole geometries selected. With these observations in mind, the set of plates shown in Figure 2.2 were modeled and their stress concentration factors were calculated.

The finite element models of the aforementioned geometries were created and analyzed using Abaqus. All geometries were subjected to a gross section tensile stress of 1 ksi along the length of the plates. The constructed models are two-dimensional and are subjected to quasi-static implicit analysis in which large deformation theory is used. The type of finite elements utilized were 8-node biquadratic plane stress quadrilaterals with

reduced integration (CPS8R, per Abaqus designation). Quadratic formulation is classically utilized in the calculation of large strain gradients, such as the ones occurring at stress risers, in elastic problems. Nevertheless, all cases described in Figure 2.2, were modeled with two mesh sizes, a base mesh size and a refined mesh size, to guarantee mesh convergence. In the base mesh size, the elements surrounding within distance $W/20$ of the hole had a maximum element size of $W/80$, and $W/20$ everywhere else. For the refined mesh size the size of the elements was halved, so the element density was approximately quadrupled. Figure 2.3 shows a comparison of the meshes utilized.

In addition to the cases selected and described in Figure 2.2, the presence of additional holes around a manhole is studied as well. Inspection access holes cut in the bottom flange of tub girders sometimes feature a small slot hole that is used to lock a door. The detail that was selected was found on design drawings provided by the state of Texas. A sample drawing of such detail is shown in Figure 2.4. To assess how the installation of those slot holes affects the fatigue performance of the manhole, an additional set of finite element models were developed. In this case finite element models of plates with a typical oval manhole 36" long by 20" wide and oval slot holes 3" by 1" wide were constructed and analyzed as in the cases described in Figure 2.2, in these cases, the varying parameter is the width of the plate (W) which different values are 33.4", 40", 50", 66.6", 100", and 200" (A/W for the inspection access hole are 0.60, 0.50, 0.40, 0.30, 0.20, and 0.10, respectively). The mesh characteristics are slightly modified for these models to accommodate the presence of the small slot hole next to the large manhole, but, as before, a base mesh and a refined mesh were used to guarantee mesh convergence. Figure 2.5 shows a sketch of the geometries modeled.

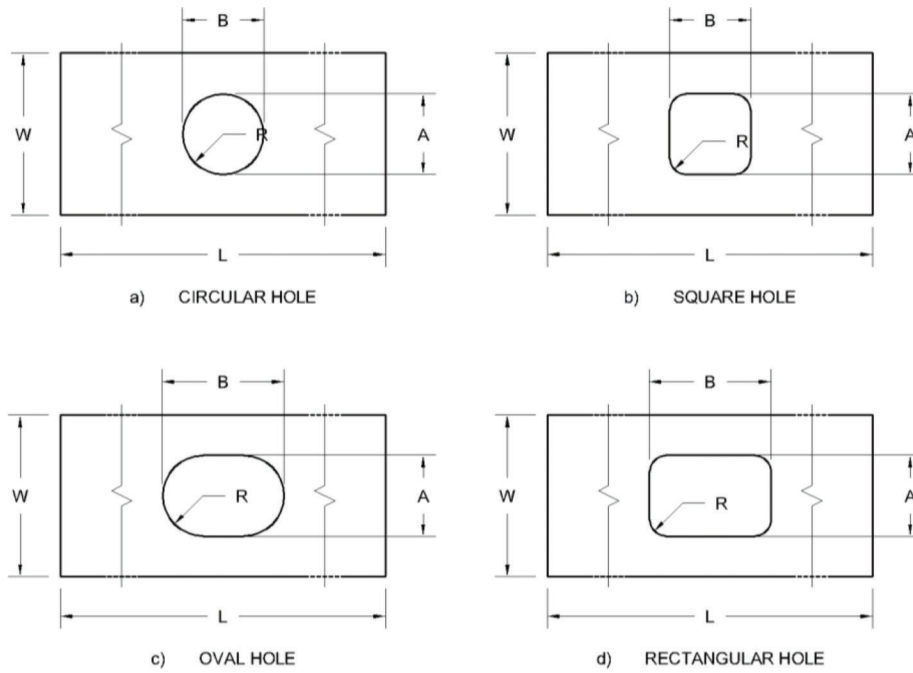


Figure 2.1 Annotated sketches of manhole and hand hole geometries modeled.

Type of Hole	A/W	B/W	R/W	
Circular	0.10	0.10	0.05	
	0.20	0.20	0.10	
	0.30	0.30	0.15	
	0.40	0.40	0.20	
	0.50	0.50	0.25	
	0.60	0.60	0.30	
	0.70	0.70	0.35	
	0.80	0.80	0.40	
	0.90	0.90	0.45	
Square	0.20	0.20	0.02	
			0.04	
			0.06	
			0.08	
			0.10	
			0.12	
	0.30	0.30	0.04	
			0.06	
			0.08	
			0.10	
			0.12	
			0.14	
	0.40	0.40	0.02	
			0.04	
			0.06	
			0.08	
			0.10	
			0.12	
0.50	0.50	0.04		
		0.06		
		0.08		
		0.10		
		0.12		
		0.14		
Square	0.50	0.50	0.16	
			0.18	
			0.20	
			0.22	
			0.24	
			0.02	
	0.60	0.60	0.04	
			0.06	
			0.08	
			0.10	
			0.12	
			0.14	
	0.70	0.70	0.16	
			0.18	
			0.20	
			0.22	
			0.24	
			0.26	
Square	0.80	0.80	0.02	
			0.04	
			0.06	
			0.08	
			0.10	
			0.12	
	0.90	0.90	0.16	
			0.18	
			0.20	
			0.22	
			0.24	
			0.26	
	Oval	0.10	0.05	0.02
				0.04
				0.06
				0.08
				0.10
				0.12
Oval	0.10	0.05	0.16	
			0.18	
			0.20	
			0.22	
			0.24	
			0.26	
	0.20	0.10	0.28	
			0.30	
			0.32	
			0.34	
			0.36	
			0.38	
	0.30	0.15	0.40	
			0.42	
			0.44	
			0.46	
			0.48	
			0.50	
0.40	0.20	0.52		
		0.54		
		0.56		
		0.58		
		0.60		
		0.62		
Rectangular	0.30	0.10	0.48	
			0.50	
			0.52	
			0.54	
			0.56	
			0.58	
	0.40	0.10	0.60	
			0.62	
			0.64	
			0.66	
			0.68	
			0.70	
	0.10	0.05	0.72	
			0.74	
			0.76	
			0.78	
			0.80	
			0.82	

Figure 2.2 Set of geometries selected for parametric study.

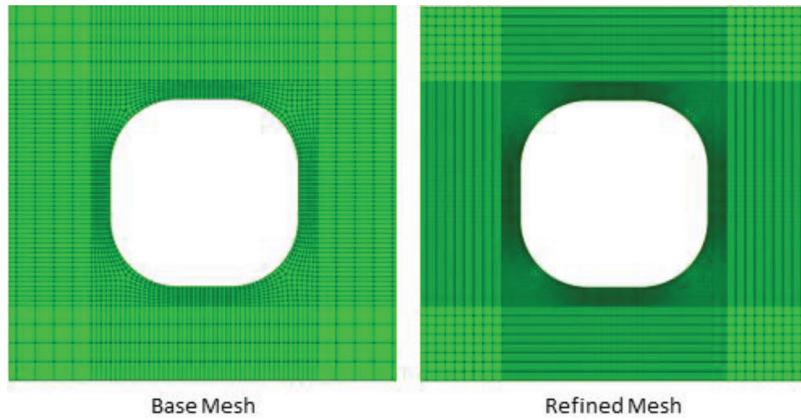


Figure 2.3 Comparison of mesh sizes used in analysis.

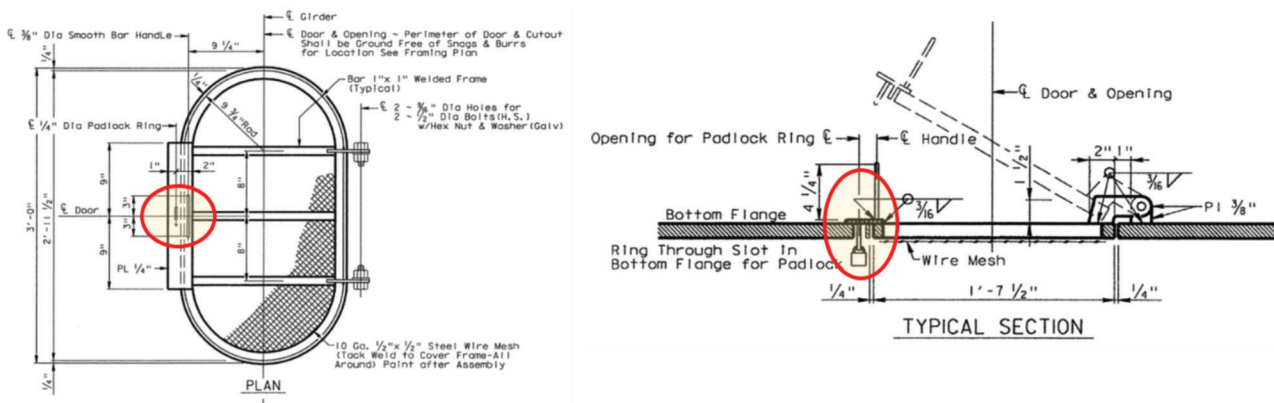


Figure 2.4 Example of tub girder inspection access hole with slot hole for lock, slot hole detail highlighted.

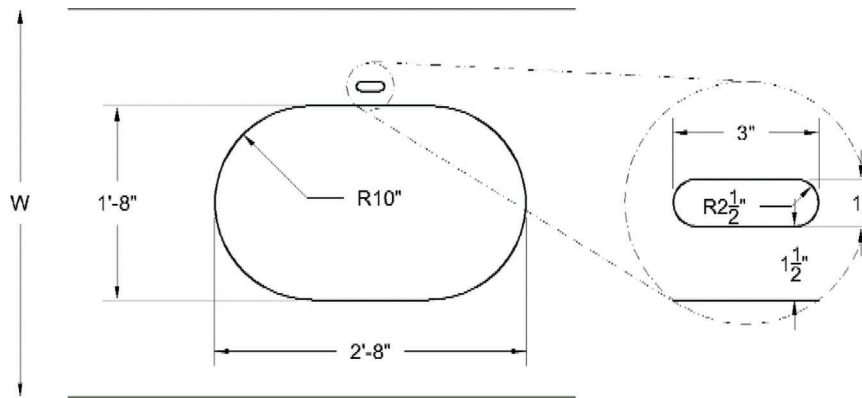


Figure 2.5 Annotated sketches of tub girder inspection access hole geometries modeled.

3. RESULTS

Since the research conducted in the current study is focused on manholes and hand holes in base metal, other variables such as residual stresses due to welding, fastener pre-tension forces, welding type, weld defects etc. do not need to be taken into account as they affect other fatigue-prone details. Thus, the load-induced fatigue performance of these details may be characterized by comparing the relative stress concentration factors to that associated with the known fatigue resistance of a plate with an open hole.

The following variables are calculated for each geometry analyzed:

- Gross section stress, σ_G : Total longitudinal force divided by the cross-sectional area of the plate without taking the hole into account. For all models this equals the applied traction of 1 ksi.
- Net section stress, σ_N : Total longitudinal force divided by the cross-sectional area of the plate in which the area of the hole is removed. Since a unit thickness was used, this corresponds to the width of the hole, A. For all models this may be calculated as follows:

$$\sigma_N = \frac{\sigma_G}{1 - A/W}$$

- Maximum tensile stress, σ_{max} : Maximum principal stress calculated in the model. Depending on the geometry of the hole the direction of the maximum principal may not be exactly parallel to the longitudinal axis of the plate.
- Stress concentration factor, SCF : The ratio between the maximum tensile stress and the net section stress, as follows:

$$SCF = \frac{\sigma_{max}}{\sigma_N}$$

In the case of open holes, the stress concentration factor is directly comparable to the ratio between the constant-amplitude fatigue threshold of smooth base metal, 24 ksi (Category A) and the constant-amplitude fatigue thresholds of the lower category. As stated above, a simple approach was used in which the “base” case assumed to be known and associated with a plate with a typical hole for a bolt, the CAFL of which is presently characterized by category D in AASHTO. Hence, a hole geometry with a stress concentration factor below 1.50 can be classified as a Category B detail ($24/16 = 1.5$), below 2.40 as a Category C detail ($24/10 = 2.4$), and below 3.43 as a Category D detail. Tables 3.1 to 3.6 summarize the results for the plate geometries described in Figure 2.2, showing in red the cases that resulted in Category D, green for Category C, and blue for Category B. The results shown are the average from two finite element models, one with the base mesh size and one with the refined mesh size. For all of the cases modeled, the maximum tensile stress values computed using the two different mesh sizes are typically within 2%; however, some

TABLE 3.1
Summary of results for circular holes.

A/W	B/W	R/W	σ_G	σ_N	σ_{max}	SCF
0.10	0.10	0.05	1.00	1.11	3.06	2.75
0.20	0.20	0.10	1.00	1.25	3.16	2.53
0.30	0.30	0.15	1.00	1.43	3.38	2.36
0.40	0.40	0.20	1.00	1.67	3.75	2.25
0.50	0.50	0.25	1.00	2.00	4.35	2.17
0.60	0.60	0.30	1.00	2.50	5.32	2.13
0.70	0.70	0.35	1.00	3.33	6.99	2.10
0.80	0.80	0.40	1.00	5.00	10.34	2.07
0.90	0.90	0.45	1.00	10.00	20.36	2.04

TABLE 3.2
Summary of results for square holes with A/W of 0.20, 0.30, 0.40, and 0.50.

A/W	B/W	R/W	σ_G	σ_N	σ_{max}	SCF
0.20	0.20	0.02	1.00	1.25	4.00	3.20
		0.04	1.00	1.25	3.34	2.67
		0.06	1.00	1.25	3.08	2.47
		0.08	1.00	1.25	2.98	2.39
0.30	0.30	0.02	1.00	1.43	4.72	3.30
		0.04	1.00	1.43	3.86	2.70
		0.06	1.00	1.43	3.53	2.47
		0.08	1.00	1.43	3.32	2.33
		0.10	1.00	1.43	3.21	2.24
		0.12	1.00	1.43	3.17	2.22
0.40	0.40	0.02	1.00	1.67	5.36	3.21
		0.04	1.00	1.67	4.38	2.63
		0.06	1.00	1.67	4.00	2.40
		0.08	1.00	1.67	3.77	2.26
		0.10	1.00	1.67	3.62	2.17
		0.12	1.00	1.67	3.54	2.12
		0.14	1.00	1.67	3.49	2.10
		0.16	1.00	1.67	3.49	2.09
0.50	0.50	0.02	1.00	2.00	5.98	2.99
		0.04	1.00	2.00	4.95	2.47
		0.06	1.00	2.00	4.52	2.26
		0.08	1.00	2.00	4.27	2.13
		0.10	1.00	2.00	4.11	2.05
		0.12	1.00	2.00	4.02	2.01
		0.14	1.00	2.00	3.97	1.99
		0.16	1.00	2.00	3.96	1.98
		0.18	1.00	2.00	3.97	1.98
		0.20	1.00	2.00	3.99	2.00
0.22	1.00	2.00	4.05	2.03		
0.24	1.00	2.00	4.18	2.09		

results showed larger differences. In Tables 3.1 to 3.6, the results in which the differences were larger than 2% are *italicized*. The same procedures were followed for the results of the tub girder inspection holes with adjacent small slot holes, which are summarized in Table 3.7.

TABLE 3.3
Summary of results for square holes with A/W of 0.60, and 0.70.

A/W	B/W	R/W	σ_G	σ_N	σ_{max}	SCF
0.60	0.60	0.02	1.00	2.50	6.77	2.71
		0.04	1.00	2.50	5.64	2.26
		0.06	1.00	2.50	5.17	2.07
		0.08	1.00	2.50	4.91	1.96
		0.10	1.00	2.50	4.75	1.90
		0.12	1.00	2.50	4.66	1.86
		0.14	1.00	2.50	4.61	1.84
		0.16	1.00	2.50	4.60	1.84
		0.18	1.00	2.50	4.62	1.85
		0.20	1.00	2.50	4.65	1.86
		0.22	1.00	2.50	4.71	1.88
		0.24	1.00	2.50	4.79	1.91
		0.26	1.00	2.50	4.88	1.95
		0.28	1.00	2.50	5.02	2.01
0.70	0.70	0.02	1.00	3.33	7.88	2.36
		0.04	1.00	3.33	6.68	2.00
		0.06	1.00	3.33	6.14	1.84
		0.08	1.00	3.33	5.86	1.76
		0.10	1.00	3.33	5.70	1.71
		0.12	1.00	3.33	5.62	1.69
		0.14	1.00	3.33	5.59	1.68
		0.16	1.00	3.33	5.59	1.68
		0.18	1.00	3.33	5.62	1.69
		0.20	1.00	3.33	5.68	1.70
		0.22	1.00	3.33	5.76	1.73
		0.24	1.00	3.33	5.86	1.76
		0.26	1.00	3.33	5.98	1.79
		0.28	1.00	3.33	6.12	1.84
0.30	1.00	3.33	6.29	1.89		
0.32	1.00	3.33	6.48	1.94		
0.34	1.00	3.33	6.74	2.02		

TABLE 3.4
Summary of results for square holes with A/W of 0.80, and 0.90.

A/W	B/W	R/W	σ_G	σ_N	σ_{max}	SCF
0.80	0.80	0.02	1.00	5.00	9.84	1.97
		0.04	1.00	5.00	8.51	1.70
		0.06	1.00	5.00	7.96	1.59
		0.08	1.00	5.00	7.52	1.50
		0.10	1.00	5.00	7.45	1.49
		0.12	1.00	5.00	7.44	1.49
		0.14	1.00	5.00	7.47	1.49
		0.16	1.00	5.00	7.53	1.51
		0.18	1.00	5.00	7.62	1.52
		0.20	1.00	5.00	7.74	1.55
		0.22	1.00	5.00	7.88	1.58
		0.24	1.00	5.00	8.04	1.61
		0.26	1.00	5.00	8.23	1.65
		0.28	1.00	5.00	8.45	1.69
0.90	0.90	0.30	1.00	5.00	8.70	1.74
		0.32	1.00	5.00	8.99	1.80
		0.34	1.00	5.00	9.33	1.87
		0.36	1.00	5.00	9.34	1.87
		0.38	1.00	5.00	9.73	1.95
		0.02	1.00	10.00	15.44	1.54
		0.04	1.00	10.00	14.83	1.48
		0.06	1.00	10.00	13.56	1.36
		0.08	1.00	10.00	13.08	1.31
		0.10	1.00	10.00	12.86	1.29
		0.12	1.00	10.00	12.82	1.28
		0.14	1.00	10.00	12.82	1.28
		0.16	1.00	10.00	12.88	1.29
		0.18	1.00	10.00	12.98	1.30
0.20	1.00	10.00	13.09	1.31		
0.24	1.00	10.00	13.28	1.33		
0.28	2.00	10.00	13.69	1.37		
0.32	3.00	10.00	14.24	1.42		
0.36	4.00	10.00	14.97	1.50		
0.40	5.00	10.00	15.96	1.60		
0.44	6.00	10.00	17.37	1.74		

TABLE 3.5
Summary of results for oval holes.

A/W	B/W	R/W	σ_G	σ_N	σ_{max}	SCF
0.10	0.12	0.05	1.00	1.11	2.68	2.41
	0.14		1.00	1.11	2.58	2.32
	0.16		1.00	1.11	2.51	2.26
	0.18		1.00	1.11	2.47	2.22
	0.20		1.00	1.11	2.44	2.19
0.20	0.22	0.10	1.00	1.25	2.91	2.33
	0.24		1.00	1.25	2.80	2.24
	0.26		1.00	1.25	2.74	2.19
	0.28		1.00	1.25	2.69	2.15
	0.30		1.00	1.25	2.65	2.12
	0.32		1.00	1.25	2.62	2.10
	0.34		1.00	1.25	2.60	2.08
	0.36		1.00	1.25	2.58	2.06
	0.38		1.00	1.25	2.56	2.05
	0.40		1.00	1.25	2.54	2.03
	0.30		0.36	0.15	1.00	1.43
0.42		1.00	1.43		2.89	2.02
0.48		1.00	1.43		2.81	1.97
0.54		1.00	1.43		2.76	1.93
0.60		1.00	1.43		2.71	1.89
0.40	0.48	0.20	1.00	1.67	3.34	2.01
	0.50		1.00	1.67	3.30	1.98
	0.56		1.00	1.67	3.20	1.92
	0.60		1.00	1.67	3.15	1.89
	0.64		1.00	1.67	3.10	1.86
	0.70		1.00	1.67	3.03	1.82
	0.72		1.00	1.67	3.01	1.81
	0.80		1.00	1.67	2.94	1.76

TABLE 3.6
Summary of results for rectangular holes.

A/W	B/W	R/W	σ_G	σ_N	σ_{max}	SCF
0.30	0.36	0.10	1.00	1.43	3.10	2.17
	0.42		1.00	1.43	3.03	2.12
	0.48		1.00	1.43	2.97	2.08
	0.54		1.00	1.43	2.92	2.04
	0.60		1.00	1.43	2.87	2.01
0.40	0.48	0.10	1.00	1.67	3.51	2.10
	0.56		1.00	1.67	3.41	2.05
	0.64		1.00	1.67	3.33	2.00
	0.72		1.00	1.67	3.26	1.96
	0.80		1.00	1.67	3.20	1.92

TABLE 3.7
Summary of results for tub girder inspection access holes with adjacent slot holes.

W	A/W	σ_G	σ_N	σ_{max}	SCF
33.40	0.60	1.00	2.69	6.93	2.57
40.00	0.50	1.00	2.11	5.81	2.76
50.00	0.40	1.00	1.72	5.00	2.90
66.60	0.30	1.00	1.46	4.42	3.02
100.00	0.20	1.00	1.27	4.01	3.17
200.00	0.10	1.00	1.12	3.78	3.38

4. DISCUSSION

4.1 Circular Holes

After examining the results obtained for the circular holes, summarized in Table 3.1, it can be accepted that the circular holes with A/W (hole width to plate width ratio) equal to 0.20 or lower should still be designated as Category D details because the stress concentration ratio is over 2.40. On the other hand, the circular holes with A/W equal to 0.30 or higher may be re-designated as Category C details since their stress concentration factors are below 2.40. In fact, the stress concentration factor for A/W equal to 0.30 is 2.36, which is almost equal to the maximum stress concentration factor for a Category C detail, 2.40. This is shown in Figure 4.1.

4.2 Square Holes

Similarly, if Table 3.2 is examined, it can also be accepted that square holes with A/W equal to 0.20 should still be designated as Category D, despite the case with R/W (fillet radius to plate width ratio) equal to 0.08 that result in a stress concentration factor equal to 2.39 (which is almost equal to 2.40, the maximum stress concentration factor for a Category C detail). Furthermore, except for the square holes with A/W equal to 0.20, all rectangular holes with R/W equal to 0.10 or higher, may be re-designated as Category C details, as shown in Figure 4.2 and Figure 4.3.

Evaluation of the results summarized in Tables 3.3 and 3.4 suggest that square holes with A/W equal to 0.60 or higher may re-designated as Category C detail unless the fillet radius is too small. Although it is possible to achieve stress concentration factors lower than 2.40 with R/W less than 0.10, it should be noticed that the stress concentration factor increases rather steeply when going from R/W equal to 0.10 to R/W equal to 0.02, as shown in Figure 4.3, suggesting that for larger holes the use of reduced fillet radius has a more marked effect than for smaller holes. This is further illustrated by the results in Tables 3.3 and 3.4, which show calculated differences larger than 2% between the two mesh sizes for small values of A/W, indicating that the strain gradients close to the hot spot are very high. For reference, when a sharp corner is modeled (fillet radius is zero), in a linear elastic analysis, the stress at the hot spot will tend to infinity precluding mesh convergence. Fortunately, requiring a fillet radius equal to 10% of the width of the plate is a requirement that will be generally be easy to implement in fabrication for most structures. It can also be noticed that for A/W equal to 0.90, it is possible to obtain stress concentration below 1.50, which suggests that the performance could be that of a Category B detail.

4.3 Oval Holes

Based on a review of the results summarized in Table 3.5, it can be concluded that all oval holes maybe considered as Category C details, except for the case in

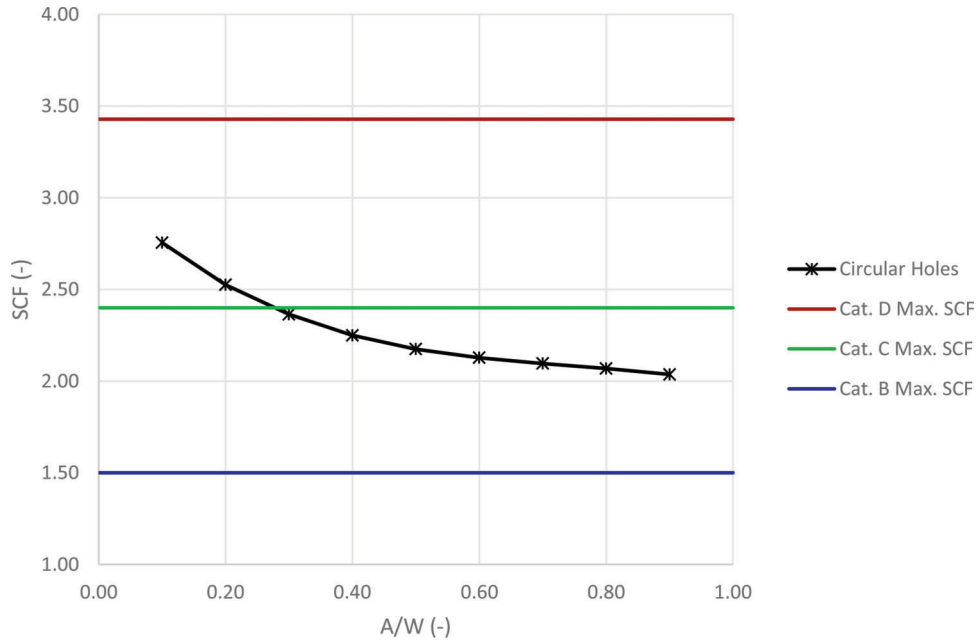


Figure 4.1 Stress concentration factor (SCF) of circular holes.

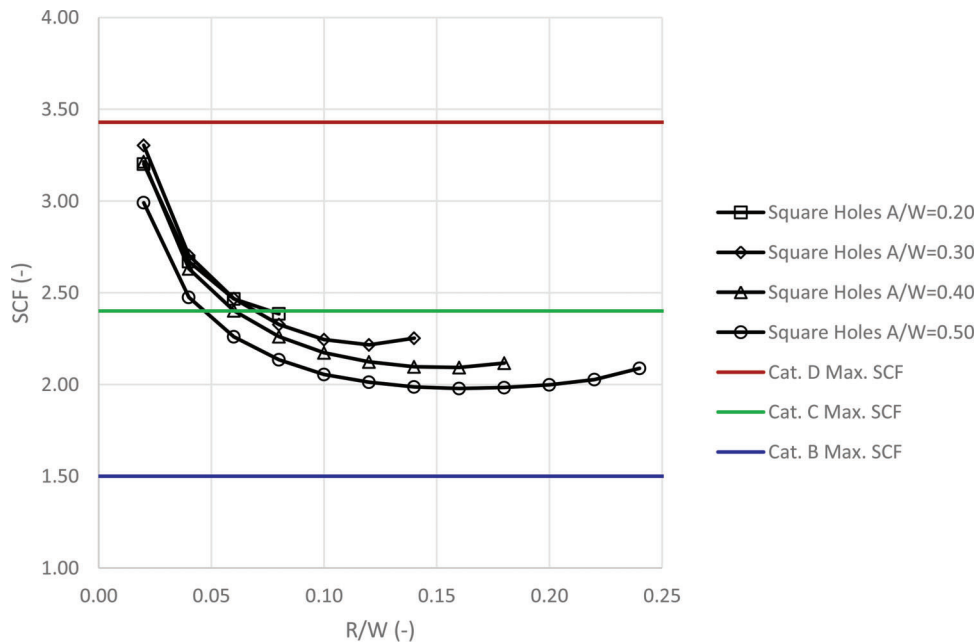


Figure 4.2 Stress concentration factor (SCF) of square holes with A/W of 0.20, 0.30, 0.40, and 0.50.

which A/W is equal to 0.10 and B/W is equal to 0.12. It is interesting to note that for circular holes with A/W less than or equal to 0.20 resulted in stress concentration factors over 2.40 (i.e., worse than that associated with the CAFL for category C). To avoid confusion, although *oval holes* with relatively small hole width to plate width ratios will most likely perform better than Category D, re-designation of oval holes with A/W less than or equal to 0.20 as Category C is not encouraged. But, it is noteworthy that based on the analysis, elongated holes, either oval or rectangular

(see Tables 3.5 and 3.6), would be expected to perform better than the circular and square holes, and that the length of an open should be equal or larger than the width of a hole.

4.4 Effect of Slots Near Inspection Access Holes

Finally, based on the results summarized in Table 3.7 of the holes described in Figure 2.5, it is evident that the fabrication of small slot holes negatively affects the fatigue performance of the adjacent tub girder inspec-

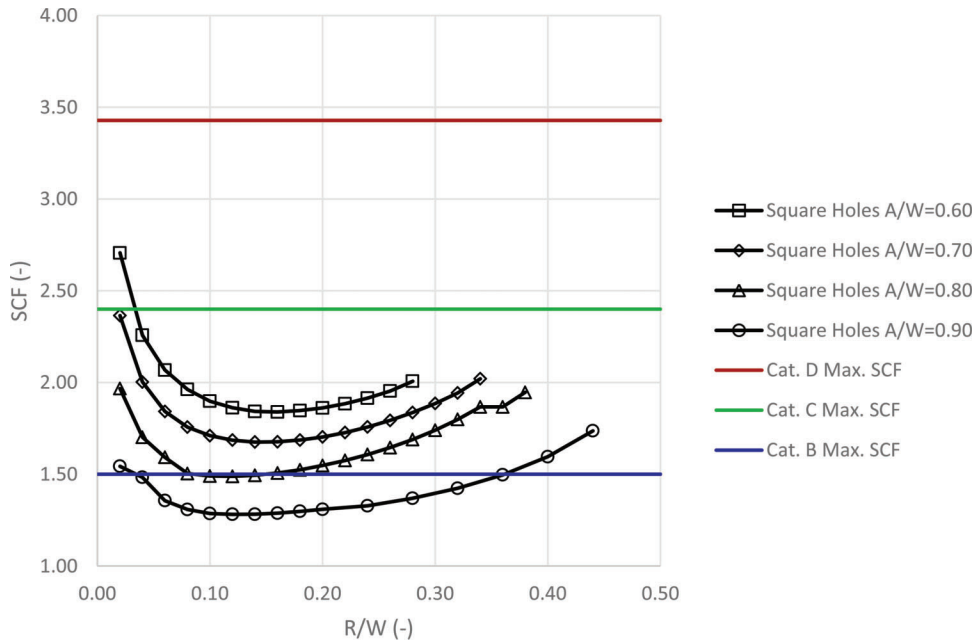


Figure 4.3 Stress concentration factor (SCF) of square holes with A/W of 0.60, 0.70, 0.80, and 0.90.

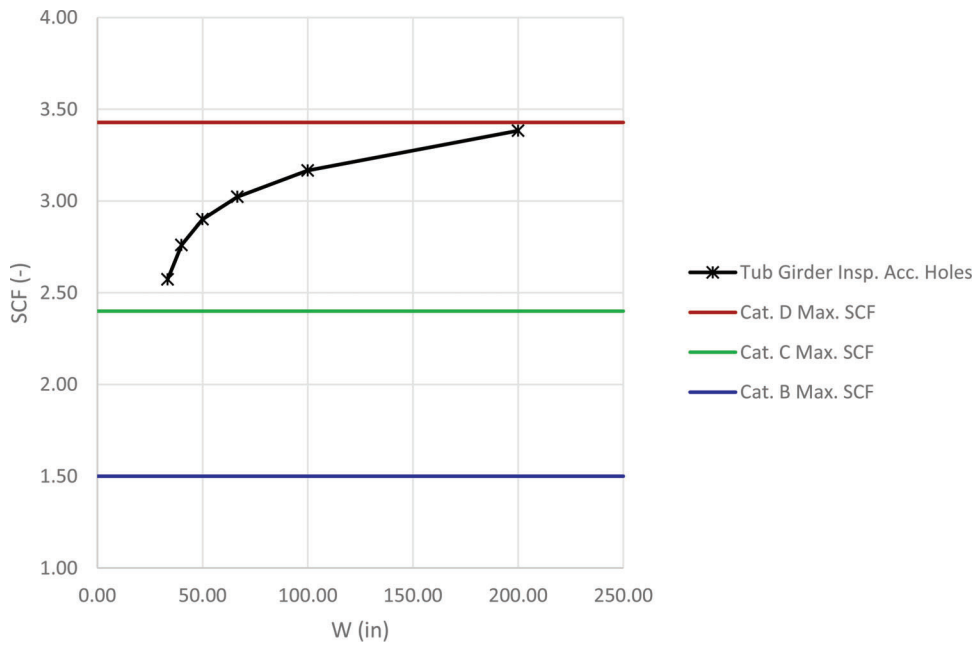


Figure 4.4 Stress concentration factor (SCF) of tub girder inspection access holes with adjacent slot holes.

tion hole. However, according to the calculated stress concentration factors, no detail is worse than Category D, as shown in Figure 4.4; but four of the modeled cases had A/W equal to 0.30 or larger, which, in the absence of an adjacent slot hole could have re-designated as category C. Hence, it is strongly recommended that these small slot holes are not installed, and other

mechanisms for locking the door to the inspection access hole are used. However, if it is absolutely necessary to install the slot hole, if installed as shown in Figure 4.5 (“in front of or behind” the access hole) the slot hole is a region where it is shielded from the path in which stress flows, and therefore does not concentrate stress.

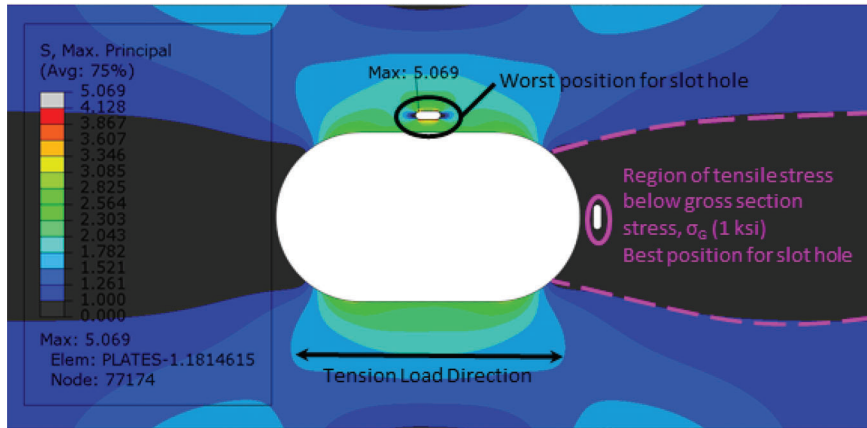


Figure 4.5 Position of slot hole and region of low tensile stress “in front of” access hole.

5. CONCLUSIONS

As shown by the results of finite element analysis of holes geometries representative of hand holes and manholes, it can be concluded that larger holes have lower stress concentration factors than smaller holes. In fact, according to the results of the previously described parametric study, the following conclusions arrive at:

- A round hole which width (or diameter) is 0.30 times the width of the plate, or larger will have a stress concentration factor below 2.40. Therefore it can be conservatively re-designated as a Category C detail.
- A square hole which width is 0.30 times the width of the plate, or larger, and its corners has been filleted to a radius equal to 0.10 times the width of the plate or larger will have a stress concentration factor below 2.40. Therefore it can be conservatively re-designated as a Category C detail.
- An oval hole, elongated in the direction of the tension load, will have lower stress concentration factor than a round hole with the same hole width to plate width ratio. Therefore it can be conservatively designated as a Category C detail.
- A rectangular hole, elongated in the direction of the tension load, will have lower stress concentration factor than a square hole with the same hole width to plate width ratio. Therefore it can be conservatively designated as a Category C detail.
- The use of slot holes in tub girder inspection access holes should be avoided unless they are installed in a region where they are shielded from tensile forces, as shown in Figure 4.5.

Additional research is needed to establish the dimensional relations in elongated holes (oval and rectangular) that lead to stress concentration factors below 2.40.

Similarly, the effect of several holes of different diameters in the same critical section should be investigated to address the issue of interacting stress concentration mechanism. During the current research it was noticed that square holes with A/W equal to 0.90 could be re-designated as a Category B detail, it may also be possible that elongated holes with A/W between 0.60 and 0.90 could be re-designated as Category B detail; however further analysis needs to be carried out. In the current study it was assumed that the hole was centered in the plate, a supplementary study is required to know how the position of the hole affects the stress concentration factor.

Finally, the best way to address the actual effects associated with the various geometries is to develop an equation for each detail type that accounts for A , W , B , and R and calculate the actual stress concentration factor (SCF) at the edge of the hole. The calculated nominal stress range would then be multiplied by the SCF and the resulting stress range compared to Category A. It is noted that standard solutions are already available for round holes. This may be useful when evaluating bridges which don't meet the limits shown in Figure 5.1, when the simplified approach is too conservative, or when trying to exploit the actual improved fatigue resistance of some geometries (i.e., those which approach Category B using the simplified approach as noted above).

Based on the conclusions and limitations of the current study, a modification to Table 6.6.1.2.3-1—Detail Categories, for Load-Induced Fatigue, Section 1—Plain Material away from Any Welding on the AASHTO LRFD Bridge Design Specification (AASHTO, 2014) is suggested, as shown in Figure 5.1.

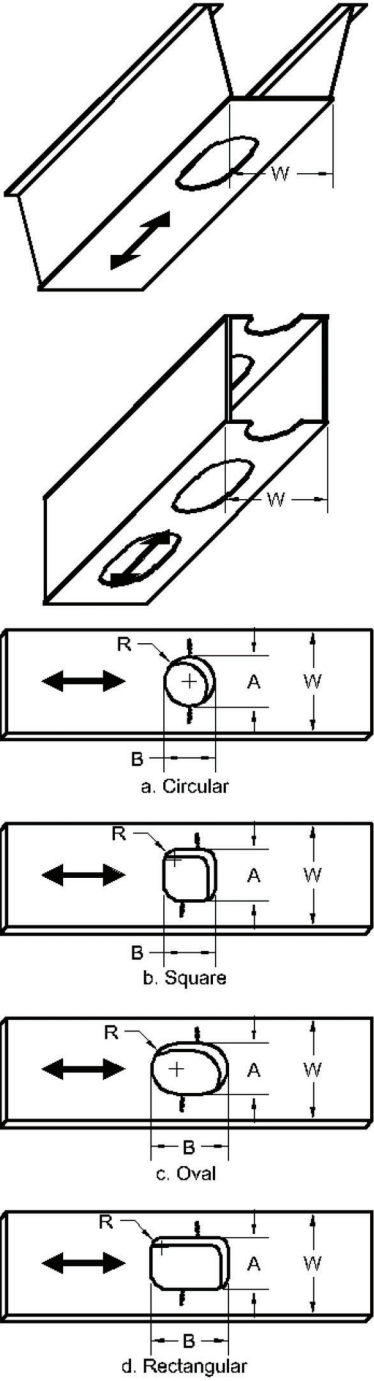
Description	Category	Constant A (ksi) ³	Threshold (ΔF) _{TH} (ksi)	Potential Crack Initiation Point	Illustrative Examples
<p>1.6 Base metal at the net section of manholes or hand holes, in which the width of the hole is at least 0.30 times the width of the plate ($A \geq 0.30W$). The geometry of the hole shall be:</p> <p>a. circular; or</p> <p>b. square with corners filleted at a radius at least 0.10 the width of the plate ($R \geq 0.10W$); or</p> <p>c. oval ($B \geq A$), elongated parallel to the primary stress range; or</p> <p>d. rectangular ($B \geq A$), elongated parallel to the primary stress range, with corners filleted at a radius at least 0.10 times the width of the plate ($R \geq 0.10W$).</p> <p>All holes shall be centered on the plate under consideration, and all stresses shall be computed on the net section.</p> <p>(Note: when other smaller open holes or holes with non-pretensioned fasteners are located anywhere within the net section of the larger hole, and minimum edge distance requirements specified in Article 6.13.2.6.6 are satisfied for the smaller holes, Condition 1.5 shall apply for all holes in that cross-section.)</p>	C	44×10^8	10	In the net section originating at the side of the hole	

Figure 5.1 Suggested modification to Table 6.6.1.2.3-1—Detail Categories, for Load-Induced Fatigue, Section 1—Plain Material away from Any Welding on the AASHTO LRFD Bridge Design Specification.

REFERENCES

- AASHTO. (2011). *The manual for bridge evaluation* (2nd ed.). Washington, DC: American Association of State Highway and Transportation Officials.
- AASHTO. (2014). *AASHTO LRFD bridge design specifications* (7th ed.). Washington, DC: American Association of State Highway and Transportation Officials.
- Brown, J. D., Lubitz, D. J., Cekov, Y. C., Frank, K. H., & Keating, P. B. (2007). *Evaluation of influence of hole making upon the performance of structural steel plates and connections* (Report No. FHWA/TX-07/0-4624-1). Austin, TX: Texas Department of Transportation.
- Kirsch, E. G. (1898). Die Theorie der Elastizität und die Bedürfnisse der Festigkeitslehre. *Zeitschrift des Vereines Dtsch. Ingenieure*, 42(29), 797–807.
- Pilkey, W. D., & Pilkey, D. F. (2008). *Peterson's stress concentration factors* (3rd ed.). Hoboken, NJ: John Wiley & Sons.

S-BRITE Center

As infrastructure continues to age, the engineers who designed and had first-hand knowledge of the then new structures (e.g., the Interstate era) eventually exit the workforce. Further, the vast majority of the infrastructure comprises structures built with older materials, design philosophies, and construction practices that are no longer discussed in the classroom. To successfully maintain the existing steel bridge inventory, expertise is needed in the areas of deterioration, fatigue, fracture, corrosion, repair/retrofit, coatings, materials, NDE, riveting, welding, and fabrication. Using Purdue's existing strengths in education and research, the Steel Bridge Research, Inspection, Training, and Engineering (S-BRITE) Center fills a growing need in the transportation industry as it relates to existing and aging steel bridges.

Additional information about the S-BRITE Center is available at <https://engineering.purdue.edu/CAI/SBRITE>.

Publication

This report was published by the S-BRITE Center at Purdue University. The full content of this technical report (in pdf and e-book formats) is available for download at <https://doi.org/10.5703/1288284316633>. In addition, a print-on-demand bound version of this report can be purchased at that location.

Open Access and Collaboration with Purdue University

The Indiana legislature established the Joint Highway Research Project in 1937. In 1997, this collaborative venture between the Indiana Department of Transportation and Purdue University was renamed as the Joint Transportation Research Program (JTRP) to reflect state and national efforts to integrate the management and operation of various transportation modes. Since 1937, the JTRP program has published more than 1,600 technical reports. In 2010, the JTRP partnered with the Purdue University Libraries to incorporate these technical reports in the University's open access digital repository and to develop production processes for rapidly disseminating new research reports via this repository. Affiliated publications have since been added to the JTRP collection, which has exceeded 1.5 million downloads.